The Structure of the Aluminium Smelting Cell Ledge

Jingjing Liu[1], Shanghai Wei[2], John J.J. Chen[3] and Mark P. Taylor[4]
1. Postdoctoral Fellow
2. Professor
3. Professor
4. Department of Chemical & Materials Engineering,
5. Research Fellow
6. Director
NZ Product Accelerator, Faculty of Engineering
All at: University of Auckland, Auckland, New Zealand
Corresponding author: jingjing.liu@auckland.ac.nz

Abstract

In aluminium smelting cells, ledges form on the cell walls. Modern cell design and control cause a suitable ledge profile to form and maintained in order to protect the cell walls from the corrosive liquids, and ensure efficient current distribution and cell heat balance. During cell operation, significant ledge freezing and melting does occur following heat balance changes due to batch operations. In the laboratory scale, a ledge formation mechanism has been studied. It shows a linkage between the rate and directional nature of ledge growth, and its structure, as affected through a superheat change. An open ledge structure can dominate the ledge material growth or melt it out quickly when the superheat either decreases or increases, respectively. This paper begins the investigation of industrial ledge samples, in terms of structure and composition primarily, to identify if this ledge formation mechanism exists in the industrial cell.

Keywords: Aluminium smelting, industrial ledge, structure.

1. Background

Cell wall integrity is critical for maintaining the cell heat balance and a safe operation of an aluminium reduction cell. In terms of integrity, we include the lining materials, such as SiC and refractory bricks etc., and the side ledge that is frozen on the walls. The ledge should be maintained in a profile which allows sufficient heat transfer through side wall (not too thick), and also protect the lining materials from the corrosive liquids (not too thin). Although the side ledge is submerged in molten liquids and is therefore not visible during the daily operation, the ledge profile can be measured as required to ensure the sufficient protection of the walls and good thermal balance of the cell. Not only the ledge and its profile that is formed on the walls is critical, the part of the ledge that extends on the cathode surface (ledge toe) has a significant impact on the current distribution if the ledge toe extends beneath the anode shadow, making the current flow path from the anode to cathode to be non-vertical since the frozen ledge is an insulating material.

Studies on ledges date from 1980s and the industrial ledge dynamic behaviours have been studied (ledge thickness and ledge profile) and discussed by many researchers in terms of heat transfer and ledge composition [1-3]. In principle, the ledge material has been traditionally considered as pure cryolite precipitating from the molten bath as the primary phase and is frozen to the walls as the temperature there drops below the bath liquidus temperature. A thin dynamic boundary layer should be formed at the ledge/bath interface in theory, where the temperature is close to bath liquidus point.

Of course in the industrial ledge, bath components such as AlF_3, CaF_2 and alumina are present in the boundary layer, and have also been found [2, 3] in the ledge itself. And recent research has

shown that ledge formation and the bath components within the ledge material have a strong impact on the ledge structure and thermal properties[4-6]. Laboratory ledge materials were used in most of these studies to shed light on its structure.

It is likely that the ledge from industrial cells is more complex in terms of composition and micro-structure, especially it is formed during transient events such as anode effect and normal cell operations such as anode setting etc. Hence, ledge formation is likely to be more complex as well. The key issue therefore is whether the structure of industrial ledge contains regions of open crystalline layers where the residual liquid is high in chiolite and alumina phases, which are inherently low melting.

In this paper, cold ledge materials sampled from a cut-out cell has been studied with a view to understand the variance of its composition and microstructure, where are compared with results from ledge formed under laboratory conditions.

2. Methodology

2.1. Investigation of the Laboratory Ledge Material

In our previous study, laboratory ledge materials were studied to understand the ledge structure and growth mechanism [6-9]. The ledge investigated in the laboratory scale showed that the bath modifiers (AlF_3, CaF_2 and alumina etc.) form different phases and morphologies when observed in the ledge among the usually dominant cryolite phase.

FigureFigure 1 show typical structures observed in the laboratory ledge. At a slow cooling rate, the first phase precipitated is the cryolite solid solution, forming a thin layer of columnar crystals at the wall surface and insulating the wall due to its much lower thermal conductivity compared with the graphite. Ca-cryolite (less than 1 %, and undetectable by XRD) precipitates out of the cryolite solid solution at a temperature below 700 °C. When new crystals continue to grow on this initial ledge layer, the lower thermal driving force for solidification causes a slower growth rate of the cryolite solid solution; thus, liquid (molten bath in the lab cell) gets a chance to be trapped among these dendritic crystals. The entrapped liquid becomes more concentrated in modifiers as the cryolitic crystals surrounding it grow in size, leaving very high ex-AlF_3 content in the entrapped liquid, whose liquidus point decreases and is much lower than the bath liquidus point.

In the portion of ledge where the actual temperature is above the liquidus point of the entrapped liquid, the entrapped liquid will stay molten and an open structure is formed, as shown in Figure 1 (c) and (c-1). In the previous work, this open structure actually has resulted in a low dimensional stability of the ledge layer when thermal balance is disturbed, i.e. a small superheat increase causes very rapid disintegration of the bulk of the ledge layer. These observations and mechanism have been investigated using the laboratory ledge. But considering the simplified thermal conditions and short-term aging of the ledge (about 1.5 hours) in the lab furnace, the industrial ledge is expected to behave differently, and some preliminary results will be reported in this paper.

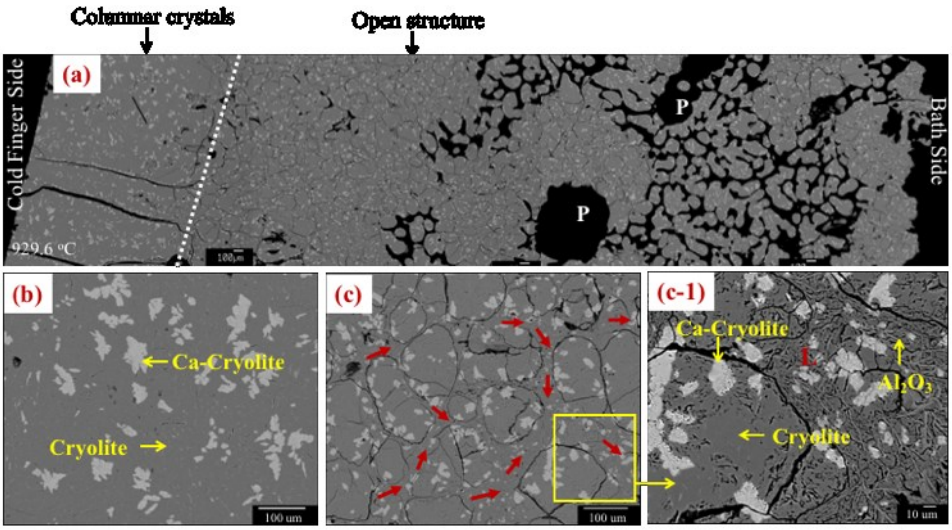

Figure 1. Structure of laboratory ledge.

2.2. Industrial Ledge-Sampling Method

The inconsistency of the ledge in an industrial cell poses a serious challenge for the ledge sampling. As we had expected and also observed during the sampling, the ledge structure varies with locations since different thermal events are occurring at different places within one cell, as indicated in the top view of a cell in Figure 2.

Figure 2. Ledge sampling locations in the cell, Location 3 is at the DUCT END.

The duct end wall ledge is observed to be more stable than the rest of the cell because no crust breaking occurs there (e.g. sampling, tapping and carbon dust removal all occur at the tap end). The Duct End ledge is therefore chosen as being representative of more matured, stable ledge

material. One large ledge section was taken from the duct end of a shut-down cell (scheduled cutout, cell life 1555 days), i.e. location 3 as shown in Figure 2.

Figure 3 shows the cross-section of the ledge profile from the wall to the interface with the liquids and the back view against the wall surface, 34 cm high and 15 cm thick. The ledge shows a great diversity in color and visual appearance. At the liquid-side surface, a thin layer of frozen electrolyte (2 mm) forms here and appears white and fine grained, while on the wall side a layer of large columnar crystals is clearly visible (about 5 mm thick, see Figure 3 (b)). The top part of the ledge appears yellow and porous which is similar to the top crust. The middle part of the ledge is a mixture of white crystals and grey (or black) colored materials. The lower part of the ledge (about 20 cm from the bottom) appears more homogeneous with no carbon inclusions.

A vertical slice of this ledge sample was cut for further study in this project, as shown in Figure 3 (d). This slice showed significant variation vertically (from cell bottom to the top) and horizontally (from side wall to the liquid-side interface). The ledge slice was further cut into 13 horizontal strips, each at a different height from bottom to the top. In this paper, the ledge slices #4, #8 and #9 are selected for the study in this paper, to provide an understanding of ledge composition and structure and comparison of the variation.

It should be pointed out that some peripheral edges of the ledge can crumble and fall off during cutting, especially at the interfaces and where it is porous. So that in slice #4, #8 and #9, some parts such as the clear crystals might have full off during the cutting. However, care was exercised to ensure minimum cross-contamination.

Another observation is that the ledge profile from the cut-out cell shows one key difference from the typical ledge profile measured in an operating cell. As shown in Figure 3 (a), a thick layer of end-wall ledge is measured at both the bath and metal level. However, the ledge is actually measured much thinner at the bath level in an operating cell, as shown in Figure 4. The explanation for this apparently thick lower ledge is revealed by the compositional analysis later but is connected with the tapping of all the aluminium from the cell prior to its removal from the potline circuit.

2.3. Analysis

Three parts of the ledge vertical section are selected for the further analysis: slice #4, slice #8, slice #9, see Figure 3 (c). Each ledge slice was split into small specimens spanning the ledge thickness. The specimens were demarcated according to their representative structure and visual appearance. For the analysis by X-ray diffraction (XRD) and Scanning Electron Microscope (SEM), the same sample was not reusable for both measurements, thus each specimen was separated into two portion and analysed by XRD and SEM respectively.

XRD for compositional analysis: XRD analysis is a commonly used method to analyze bath composition in the aluminium smelting industry by quantifying the phases formed at room temperature. The ledge specimen was ground into a fine powder to ensure its homogeneity. As developed for the bath material [10], XRD scan was conducted in the 2θ range of 10 – 80°, with a step of 0.02° for the phase quantitative analysis, Rietveld refined using PANalytical's HighScore Plus software [11]. In this paper, the phases detected by the XRD are compared directly to show the compositional variation, which will eliminate the error of the deduction from phases to bath compounds.

SEM for microstructural analysis: The ledge specimen was mounted in epoxy resin, then polished for metallographic examination and microanalysis. SEM (FEI Quanta 200 F model) and Energy Dispersive X-ray Spectroscopy (EDS) were used for the microstructure morphology and

phase identification respectively, and further confirmed by combining the compositional analysis. The analysis method details can be found in previous work [6, 9].

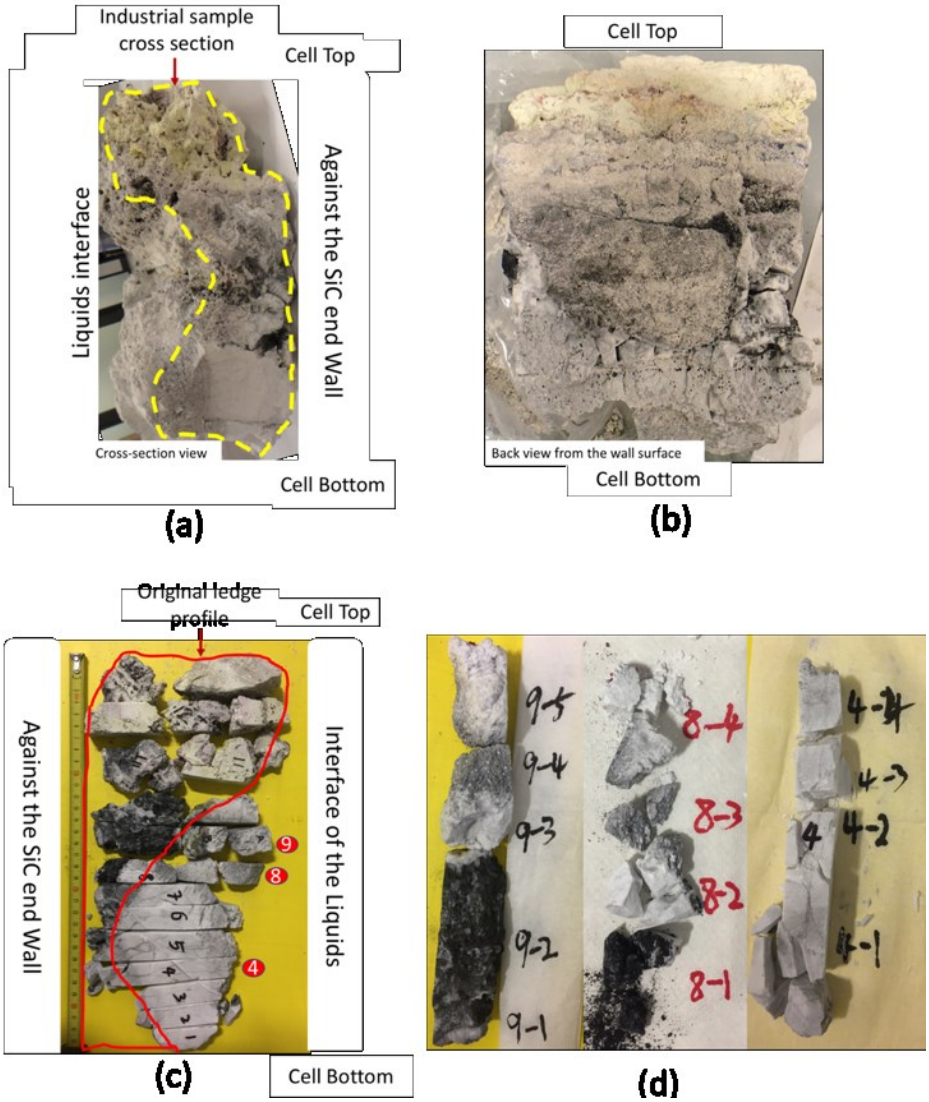

Figure 3. Ledge sample from the DUCT END (a) Cross-section of the Ledge block; (b) Back view of the Ledge block, against the wall surface; (c) Ledge vertical section cut from the ledge block; (d) Ledge specimens studied in this paper.

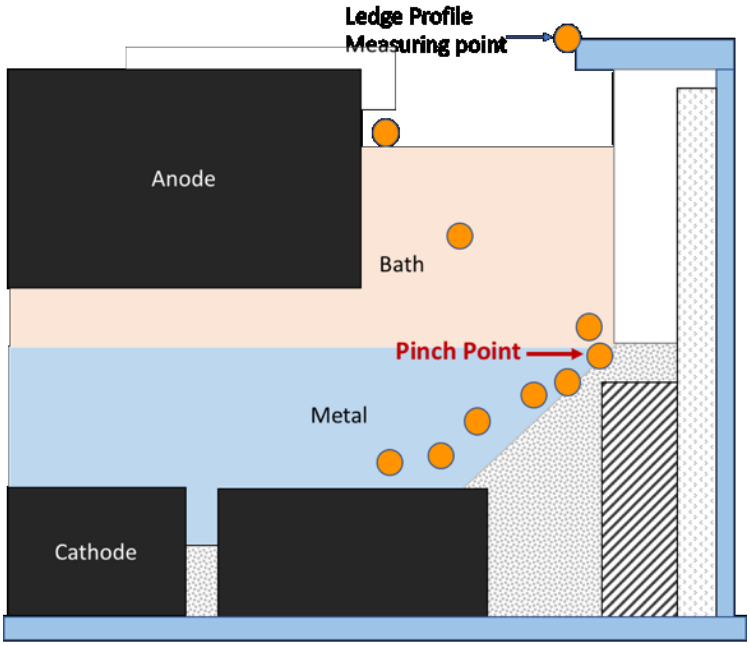

Figure 4. Typical end-wall ledge profile measured in an operating cell in a smelter, indicated by the orange dots.

3. Results and Discussion

3.1. Compositional analysis

Table 10 gives the composition of the phases in the ledge specimens determined by XRD. Each ledge specimen, i.e. slice #4, slice #8 and slice #9 are split into pieces as shown in Figure 3 (d) As observed in the table there is a wide variation over the full range of specimens. ***Slice 4*** exhibits relatively minimum variation in composition from the sidewall to the liquid-side surface, but with higher chiolite content up to 52 % compared to the conventional bath composition. ***In slice 8***, the chiolite content increases from the wall side (13 %) to the liquid-side interface (44.3 %), and a similar composition to Slice 4 is found when the ledge is close to the liquid side, i.e. specimen # 8_3 (39.3 % chiolite) and specimen # 8_4 (44.3 % chiolite). ***In slice 9***, near the side wall the ledge (specimen 9_1) contains an undetectable amount of chiolite: 0 % chiolite next to the wall surface, with the highest amount of CaF_2 in specimen 9_1. There is a measurable amount of chiolite in this slice - ledge specimen # 9_2 (3.7 %). Also, in slice 9, towards the liquid side a higher chiolite content is measured, very similar to column 4.

It should be pointed out that despite the dark colour of several specimens, the graphite content measured by XRD was quite low. Amorphous carbon phases could increase the amount of carbon assayed however.

Considering the unexpected frozen sample thickness at the metal level and the very high chiolite content apparently concentrated into the metal level parts of the sample, it became clear that a substantial proportion of the specimens in Table 1, including all of slice 4 and the liquid facing specimens of slices 8 and 9, is bath frozen onto the original ledge, mostly at the metal level and with a thinner layer at the bath level. This cooling bath was displaced downward by the removal of all aluminium at cutout, and would have been the last bath to freeze in the cutout cell as it is in the proximity of the cathode. The original ledge profile has been estimated in this sample and is outlined in red, As shown in Figure 3 (b), based on the composition of chiolite in each specimen.

The visual appearance of this frozen bath is fine grained compared with the larger, crystalline appearance of the actual ledge.

More detailed examination was then conducted on the original ledge specimens identified in red in Table 1, using specimen 8_1, specimen 9_1 and specimen 9_2. Some variations are observed between these three specimens, with specimen 9_1 being the purest in cryolite and with no Ca-cryolite detected by XRD. Cryolite is the dominant phase in all three original ledge samples, with chiolite and Ca-cryolite content varying among the samples, but with relative consistency of CaF_2 and corundum. In specimen #8_1, the highest chiolite content is found to be 13 % although this is still part of the original ledge. This ledge is similar to the open crystalline structure composition of the laboratory ledge [7].

Table 15. Compositional phase analysis by XRD.

Sample#	Phase content						
	Cryolite	Chiolite	$Na_2Ca_3Al_2F_{14}$	CaF_2	Corundum	Gamma-Al_2O_3	Graphite
9_1	96.2	0	0	2.2	1.6	0	0
9_2	88.7	3.7	4	0.1	2.7	0	0.8
9_3	51.2	39.6	8.6	0	0.6	0	0
9_4	43.3	46.3	8.6	0.1	0.9	0.8	0
9_5	48.9	39.2	8.8	0.5	1.1	1.4	0
8_1	80.4	13	3.3	0.1	1.7	0	1.6
8_2	59.5	29.8	9.6	0	1.1	0	0
8_3	49.7	39.3	8.7	0.2	1.2	0.9	0
8_4	45.6	44.3	6.5	0.9	1.3	1.4	0
4_1	52.4	37.9	7.6	0.5	1.5	0	0
4_2	39	52.4	7.7	0.1	0.8	0	0
4_3	55.8	34.9	8.9	0	0.3	0	0
4_4	49.1	40.3	9.4	0.1	1.1	0	0

3.2. Microstructural Analysis

The industrial ledge samples exhibit more diversity in their microstructures compared to the laboratory ledge microstructures. Figure 5 and Figure 6 show representative microstructures for specimens 9_1 and 8_1 respectively. Carbon dust inclusions are found in most of the industrial ledge as also measured by EDS, and the grain size of cryolite and chiolite in the industrial ledge appear larger than in the laboratory ledge.

Both the industrial ledge and the laboratory ledge have a thin layer of clear columnar crystals forming at the (cold) wall surface, about 5 mm thick in the industrial ledge shown in Figure 5 and 2 mm in the laboratory ledge shown in Figure 1. In the industrial cell, the total thermal gradient across the side wall ranges from approximately 400 °C at the silicon carbide brick to 960 °C at the molten bath, i.e. the bath liquidus point. In comparison, the temperature drop across the laboratory ledge is only from 929 °C at the graphite cold finger to 958 °C at the molten bath. Therefore, the greater thermal gradient in the industrial cells can cause initial cryolitic crystal to grow into a thicker layer and with bigger grains in the industrial ledge. Another difference is that in the laboratory ledge, the clear columnar crystals are composed of cryolite and Ca-cryolite. However, in the industrial cell, the Calcium phase has mainly precipitated as pure CaF_2, due to the lower ledge temperature there (below 700 °C). In the laboratory cell the whole ledge remains above 929 °C and only very small amount of Ca-cryolite phase precipitate from the cryolite solid solution (outside of the XRD detection limit).

After the columnar crystalline layer ends, crystals continue to grow but are not aligned in the solidification direction and are observed to have inclusions of carbon dust (C+S) and alumina in the industrial ledge, as shown in Figure 5. The main phases in the crystals are Cryolite with fine

Ca-cryolite and CaF_2 precipitates dispersed all over the crystalline area (see Figure 5 (a)). Alumina appears as corundum platelets, usually mixed with Carbon dust, Cryolite and Ca-cryolite, in regions between the cryolite crystals which contain a higher porosity.

With crystals growing towards the direction of the bath side, more carbon dust inclusions dispersed in the whole sample, as shown in Figure 6 (a). The carbon dust is embedded in the ledge material, as a mixture of Cryolitic crystals, chiolite crystals, alumina platelets and carbon particles. Figure 6 (b)/(c)/(e) show typical mixture zones observed in the ledge. This mixture has high porosity, and the crystals grow into smaller grain sizes. Also, some crystals are rounded, possibility due to partial dissolution by surrounding liquid during solidification. The larger crystals are Cryolite and Ca-cryolite as found in the crystalline layer. However, in the porous mixture zone, chiolite appears along with the Cryolite phases. No difference can be observed between these two phases under SEM, but the EDS detection clearly shows the phase difference.

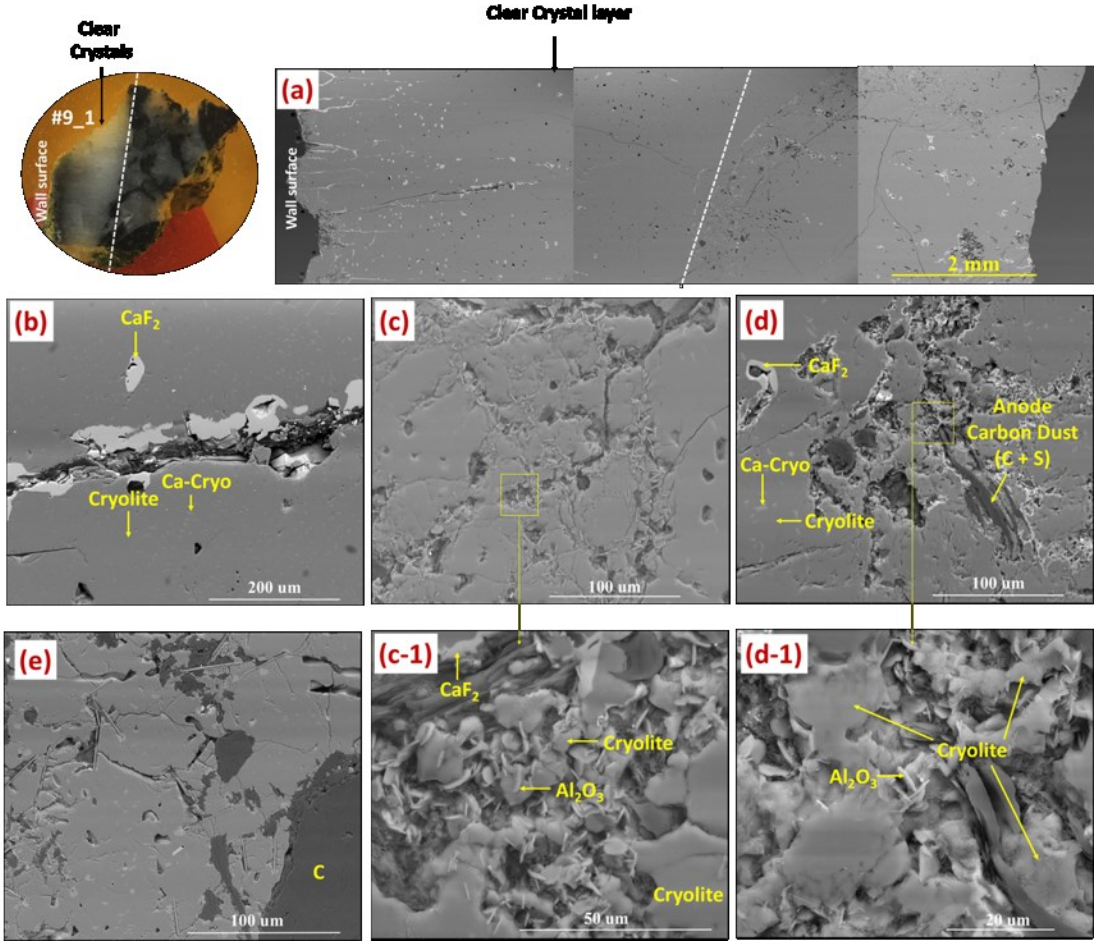

Figure 5. Typical structure of ledge specimen 9_1.

The appearance in Figure 5 of many chiolite crystals in these 'mixed' zones between the larger cryolite grains corresponds with the 13 % chiolite in this sample detected by XRD. However, the porous structure in the mixture zone has a different morphology from the simpler open structure layer in the laboratory ledge even though chiolite and alumina have both appeared. The difference in the morphology could be due to the presence of significant amounts of carbon dust particles, but equally it could be influenced by the greater temperature gradient between the wall and the molten bath in the industrial cell and also the much greater aging period of the industrial ledge.

Despite the difference in morphology observed here, it is certain that the presence of chiolite and alumina in the 'mixed' zones in specimen 8_1 bears a striking similarity to the open crystalline layer composition in the laboratory samples. The effect of the high modifier composition of the mixed zones on the local liquidus point within these sections of ledge will also be similar.

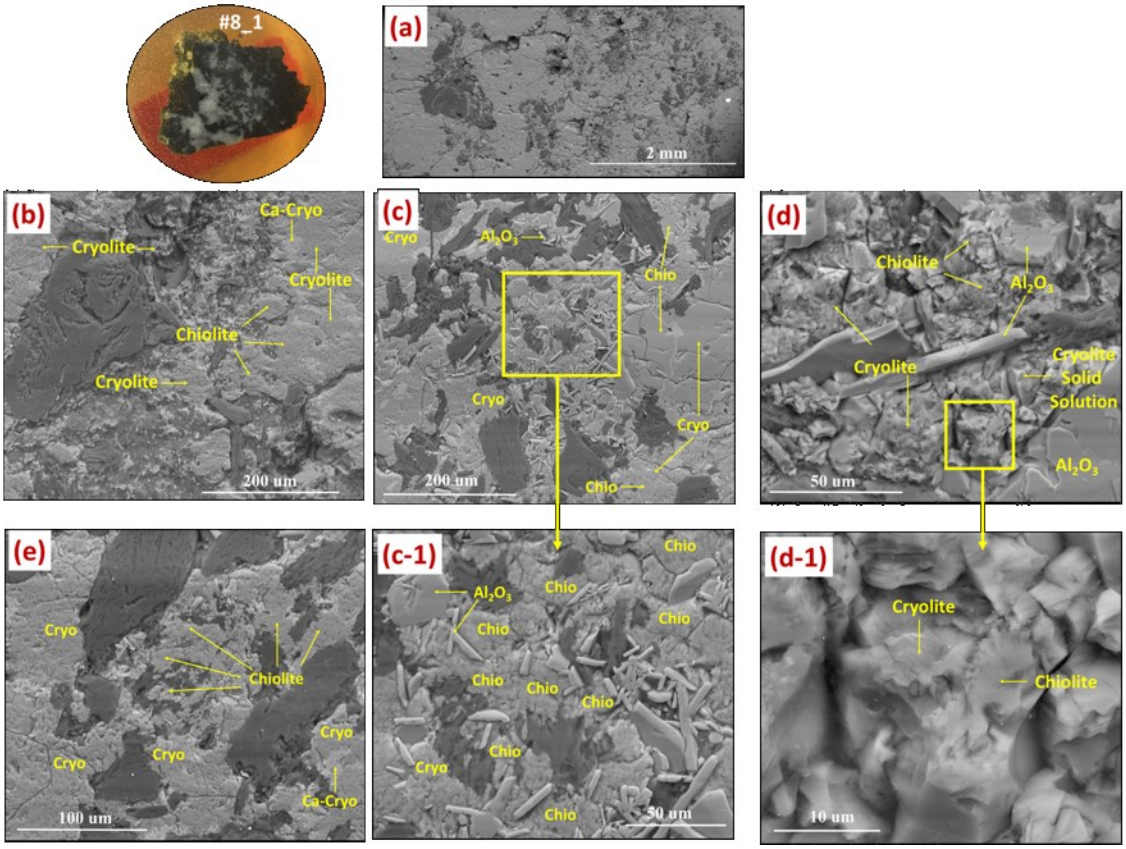

Figure 6. Typical structure of ledge specimen 8_1.

4. Conclusions

Several industrial ledge specimens obtained from a scheduled cut-out cell have been analysed and compared with laboratory formed ledge in terms of composition and micro-structure. The following findings are evident at this early stage in the investigation:

- As expected, industrial ledge shows more complexity, such as the inclusions of carbon dusts through the ledge.
- Industrial ledge grains grow into a bigger size and with a slightly thicker 'cold face' columnar layer. The thermal gradient across industrial ledge is much greater than lab-scale ledge, which could drive both of these effects.
- In one sample studied here, the interaction with the carbon dust has changed the open porous structure in the industrial ledge. Alumina phase forms as corundum platelets in the porous mixture zone together with chiolite.
- No obvious liquid channels have been observed between the larger cryolite crystals as were observed in the laboratory ledge open crystalline layer. However, it must be noted that the laboratory ledge was only maintained at temperature for about 1.5 hrs, and is therefore far away from its final chemical balance. The industrial ledge, by comparison has been aging at cell temperature for many operating days. This is probably long enough for the ledge to reach chemical balance to a greater extent. Liquid channels would then be taken up by the cryolite and chiolite crystal growth into the mixed zones, creating a different apparent morphology for the open structure layer.

5. Future plan:

This work has provided us with a first insight into industrial ledge structure. The next step is to develop a systematic method to investigate industrial ledge more thoroughly at different locations and under different cell conditions.

Based on the compositional and structural findings, future work will involve examining the thermochemical properties of the ledge materials as well as the structure, and their impacts on the cell wall heat balance.

6. Acknowledgement

MBIE funding is gratefully acknowledged for this work, under Grant UOAX1308. Support from NZAS smelter and Dr Hasini Wijayaratne at LMRC are much appreciated.

7. References

1. Mark P. Taylor, Barry J. Welch and Jeffrey T. Keniry. Influence of changing process conditions on the heat transfer during the early life of an operating cell, *Light Metals* 1983, 437-447.
2. Jomar Thonstad and Sverre Rolseth. Equilibrium between bath and side ledge, *Light Metals* 1983, 415-424.
3. X. Liu: 'Thermochemistry of electrolyte, sludge/ridge, ledge and cell cover', *Fifth Australasian Aluminium Smelter Technology Workshop*, Sydney, Australia, Oct 1995.
4. Ata Fallah-Mehrjardi, P.C. Hayes, and E. Jak. Investigation of freeze-linings in aluminum production cells, *Metallurgical and Materials Transactions B*, 2014. Vol. 45 (4), 2014, 1232-1247.
5. Asbjørn Solheim and L. I. R. Stoen, On the composition of solid deposits frozen out from cryolitic melts, *Light Metals* 1997, 325-332.
6. Jingjing Liu, Ata Fallah-Mehrjardi, Denis Shishin, Evgueni Jak, Mark Dorreen, Mark Taylor, Investigation of the Influence of Heat Balance Shifts on the Freeze Microstructure and Composition in Aluminum Smelting Bath System: Cryolite-CaF_2-AlF_3-Al_2O_3, *Metallurgical and Materials Transactions B*, Vol. 48 No. 6 (2017), 3185-3195.
7. Jingjing Liu, Mark Taylor and Mark Dorreen, Observations of freeze layer formation during heat balance shifts in cryolite-based smelting bath, *International Journal of Materials Research*, Vol. 108 No.6 (2017), 507-514.
8. Jingjing Liu, Mark Taylor and Mark Dorreen, Response of Cryolite-Based Bath to a Shift in Heat Input/output Balance, *Metallurgical and Materials Transactions B*, Vol. 48(2) (2017), 1079-1091.
9. Jingjing Liu, Mark Taylor and Mark Dorreen, Responses of Lithium-Modified Bath to a Shift in Heat Input/Output Balance and Observation of Freeze-Lining Formation During the Heat Balance Shift, *Metallurgical and Materials Transactions B*, 49(1) (2018), 238-251.
10. Nursiani Indah Tjahyono, Tania Groutso, David S. Wong, Pascal Lavoie, Mark P Taylor. Improving XRD analysis for complex bath chemistries–investigations and challenges faced, *Light Metals* 2014, 573-578.
11. PANalytical, B., *'Pert HighScore Plus software, version 3.0 e.* Almelo: Netherlands, 2012.